atoms

IMPACT FACTOR 1.7

CITESCORE 2.7

Article

Exploring the Nuclear Chart via Precision Mass Spectrometry with the TITAN MR-TOF MS

Annabelle Czihaly, Soenke Beck, Julian Bergmann, Callum L. Brown, Thomas Brunner, Timo Dickel, Jens Dilling, Eleanor Dunling, Jake Flowerdew, Danny Fusco et al.

Special Issue

Advances in Ion Trapping of Radioactive Ions

Edited by

Dr. Maxime Brodeur

MDPI

https://doi.org/10.3390/atoms13010006

atoms

MDPI

Article

Exploring the Nuclear Chart via Precision Mass Spectrometry with the TITAN MR-TOF MS

Annabelle Czihaly [1,2,*], Soenke Beck [3,4], Julian Bergmann [3], Callum L. Brown [5], Thomas Brunner [1,6], Timo Dickel [3,4], Jens Dilling [1,7], Eleanor Dunling [1], Jake Flowerdew [1,8], Danny Fusco [1,9], Leigh Graham [1], Zach Hockenbery [1,6], Chris Izzo [1], Andrew Jacobs [1,7], Brian Kootte [1,10], Yang Lan [1,7], Stephan Malbrunot-Ettenauer [11], Fernando Maldonado Millán [1], Ali Mollaebrahimi [1,3,4], Erich Leistenschneider [1,7], Eleni Marina Lykiardopoulou [1,7], Ish Mukul [1], Stefan F. Paul [1,12], Wolfgang R. Plaß [3,4], Moritz Pascal Reiter [1,3,5], Christoph Scheidenberger [3,4,13], James L. Tracy, Jr. [1] and A. A. Kwiatkowski [1,2]

1 TRIUMF, 4004 Wesbrook Mall, Vancouver, BC V6T 2A3, Canada; thomas.brunner@mcgill.ca (T.B.); dillingj@ornl.gov (J.D.); edunling@triumf.ca (E.D.); jake.anthony.darri.flowerdew@cern.ch (J.F.); danny_fusco46@hotmail.com (D.F.); leighgraham9@gmail.com (L.G.); zhockenbery@gmail.com (Z.H.); izzo@frib.msu.edu (C.I.); a.jacobs237@gmail.com (A.J.); brian.a.kootte@jyu.fi (B.K.); yanglan.physics@gmail.com (Y.L.); maldonado@triumf.ca (F.M.M.); amollaebrahimi@triumf.ca (A.M.); erichleist@lbl.gov (E.L.); mlykiardopoulou@lbl.gov (E.M.L.); ishmukul@gmail.com (I.M.); stefan.paul@triumf.ca (S.F.P.); mreiter@exseed.ed.ac.uk (M.P.R.); jamesltracyjr@gmail.com (J.L.T.J.); aniak@triumf.ca (A.A.K.)
2 Department of Physics and Astronomy, University of Victoria, 3800 Finnerty Road, Victoria, BC V8P 5C2, Canada
3 Department of Physics, Justus-Liebig-Universität Gießen, Heinrich-Buff-Ring 16, 35392 Gießen, Germany; s.beck@gsi.de (S.B.); julian.bergmann@physik.uni-giessen.de (J.B.); t.dickel@gsi.de (T.D.); wolfgang.r.plass@exp2.physik.uni-giessen.de (W.R.P.); c.scheidenberger@gsi.de (C.S.)
4 GSI Helmholtz Centre for Heavy Ion Research Planckstraße 1, 64291 Darmstadt, Germany
5 School of Physics and Astronomy, The University of Edinburgh, Old College, South Bridge, Edinburgh EH8 9YL, UK; callum.brown@ed.ac.uk
6 Department of Physics, McGill University, 845 Rue Sherbrooke O, Montréal, QC H3A 2T8, Canada
7 Department of Physics and Astronomy, The University of British Columbia, 325 - 6224 Agricultural Road, Vancouver, BC V6T 1Z1, Canada
8 Department of Physics and Astronomy, University of Calgary, 2500 University Drive NW, Calgary, AB T2N 1N4, Canada
9 Department of Physics and Astronomy, University of Waterloo, 200 University Avenue W, Waterloo, ON N2L 3G1, Canada
10 Department of Physics and Astronomy, University of Manitoba, 30A Sifton Road, Winnipeg, MB R3T 2N2, Canada
11 CERN, Esplanade des Particules 1, 1211 Geneva 23, Switzerland; sette@triumf.ca
12 Department of Physics and Astronomy, Heidelberg University, Grabengasse 1, 69117 Heidelberg, Germany
13 Helmholtz Forschungsakademie Hessen für FAIR (HFHF), GSI Helmholtzzentrum für Schwerionenforschung, Campus Gießen, 35392 Gießen, Germany
* Correspondence: aczihaly@triumf.ca

Abstract: Isotopes at the limits of nuclear existence are of great interest for their critical role in nuclear astrophysical reactions and their exotic structure. Experimentally, exotic nuclides are challenging to address due to their low production cross-sections, overwhelming amounts of contamination, and lifetimes of typically less than a second. To this end, a Multiple-Reflection Time-of-Flight mass spectrometer at the TITAN-TRIUMF facility was built to determine atomic masses. This device is the preferred tool to work with exotic nuclides due to its ability to resolve the species of interest from contamination and short measurement cycle times, enabling mass measurements of isotopes with millisecond half-lives. With a relative precision of the order 10^{-7}, we demonstrate why the TITAN MR-TOF MS is the tool of choice for precision mass surveys for nuclear structure and astrophysics. The capabilities of the device are showcased in this work, including new mass measurements of short-lived tin isotopes ($^{104-107}$Sn) approaching the proton dripline

check for updates

Academic Editor: Kirill Tuchin

Received: 31 August 2024
Revised: 4 October 2024
Accepted: 3 January 2025
Published: 9 January 2025

Citation: Czihaly, A.; Beck, S.; Bergmann, J.; Brown, C.L.; Brunner, T.; Dickel, T.; Dilling, J.; Dunling, E.; Flowerdew, J.; Fusco, D.; et al. Exploring the Nuclear Chart via Precision Mass Spectrometry with the TITAN MR-TOF MS. *Atoms* **2025**, *13*, 6. https://doi.org/10.3390/atoms13010006

as well as ^{89}Zr, ^{90}Y, and ^{91}Y. The last three illustrate how the broadband surveys of MR-TOF MS reach beyond the species of immediate interest.

Keywords: mass spectrometry; proton dripline; time-of-flight mass spectrometry; ion traps; radioactive ion beams; experimental nuclear physics

1. Introduction

The ratio of protons to neutrons as well as their total number determines the nuclear properties of any nuclide. The limits of stability or the point of being nuclear unbound are called the proton and neutron driplines. To understand the evolution of nuclear structure, and therefore the subatomic forces at play, is an outstanding challenge of intrinsic interest that also impacts studies of, for example, nuclear astrophysics. To approach the driplines experimentally invokes a number of obstacles: low production cross-sections, substantial contamination, and short half-lives. High-sensitivity, -purification, and -speed methodologies are required. These traits characterize Multiple-Reflection Time-Of-Flight Mass Spectrometers (MR-TOF MSs).

The MR-TOF MS [1,2] at TRIUMF's Ion Trap for Atomic and Nuclear science (TITAN) [3] facility was constructed to focus on mass surveys to benefit studies of nuclear structure and nuclear astrophysics, where the required relative precisions are 10^{-6} and 10^{-7}, respectively. In this quest, the TITAN MR-TOF MS has reached precisions down to 9×10^{-8} [4], removed contamination up to 10^{8} [1] times greater than the species of interest, and achieved sensitivities of rates as low as 0.007 detected ions per second [5]. Consequently, experiments focusing on driplines occur increasingly frequently at the TITAN facility.

To this end, we detail an experiment aimed at exploring the nuclear structure of neutron-deficient tin isotopes towards the proton dripline. Herein, we report mass determinations of $^{104-107}$Sn, showcasing how the MR-TOF MS can be used to reduce contamination and obtain meaningful precisions in less than ten hours of runtime. In addition, we document simultaneous mass measurements of ^{89}Zr, ^{90}Y, and ^{91}Y. These three were measured due to the broadband (i.e., non-resonant) technique of the MR-TOF MS.

2. Experimental Overview

The TITAN MR-TOF MS is based on the established setup Giessen-GSI FRS MR-TOF [6–8]. Similar devices are employed at, for example, RIKEN in Japan [9], CERN in Switzerland [10], and GSI in Germany [6], with typical relative precisions of 10^{-7}, although better values can be achieved [11]. Recent exploits of the TITAN MR-TOF MS include measuring exotic neon isotopes [12], neutron-rich scandium isotopes [13], neutron-deficient ytterbium [14], and neutron-deficient nuclei in the $Z = 70$–82 region [15].

Radioactive ion beams (RIBs) are produced via the Isotope Separation On-Line (ISOL) method, by impinging a 480 MeV proton beam onto a thick target, causing fragmentation and spallation reactions. The radionuclides diffuse out of the ≈2000 °C target and are ionized by one of three ion sources at ISAC-TRIUMF [16]. For the neutron-deficient tin experiment, a proton beam current of 55 μA was used, incident on a tantalum target, and the Sn isotopes were selectively ionized by TRIUMF's Resonant Laser Ion Source (TRILIS) [17]. The beam is then sent through a dipole magnet, with a resolving power of approximately 2500 [16], eliminating species differing in their ratio of mass number to charge state.

The RIB is then transported to TITAN's helium-gas-filled Radio Frequency Quadrupole (RFQ) ion trap [18]. The beam is cooled via successive collisions with an inert buffer gas with the RF field providing transverse confinement. An electrostatic gradient transfers the ions into the bunching region, where the beam is accumulated and then extracted as ion bunches, which are subsequently sent to the MR-TOF MS.

The MR-TOF MS [1] is composed of two main sections: a preparation section and an analyzer section (see Figure 1). The preparation system is made of a series of helium-buffer-gas-filled RFQs [19]. The bunched beam passes through the input RFQ ion guide, through the RFQ switch-yard, past the transfer RFQ, and into the preparation trap (a linear Paul trap), where it is re-cooled. Next, the beam emittance is shaped in the injection trap before injection into the analyzer section.

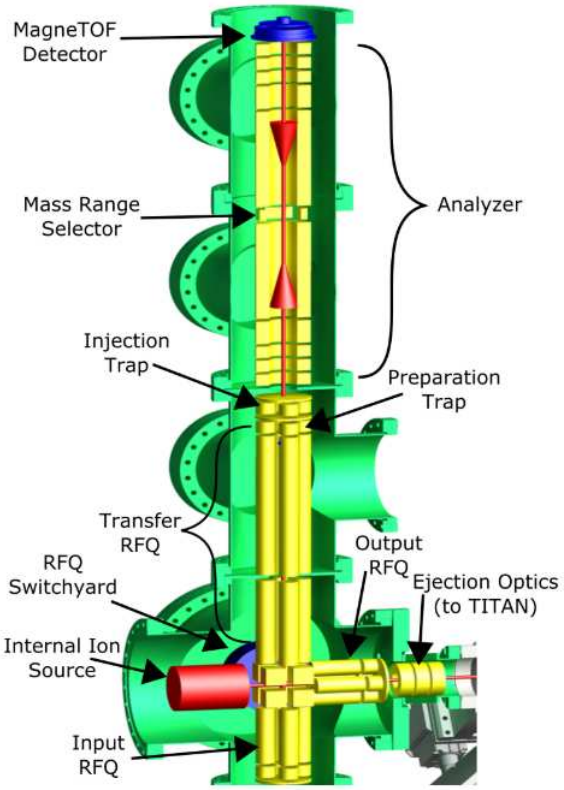

Figure 1. Schematic of the TITAN MR-TOF MS, highlighting primary components including the internal ion source, RFQ switch-yard, and analyzer. The unique combination allows the TITAN MR-TOF MS to merge calibrants with RIB and to act as its own beam purifier.

The analyzer section is made of a pair of electrostatic mirrors, each with four cylindrical electrodes, separated by a drift tube. A dynamic Time Focus Shift (TFS) is performed with the electrostatic mirror electrodes to align the bunch's time focus with the downstream detector to maximize the temporal resolution. Each subsequent turn (i.e., after the first TFS turn) is an isochronous turn (IT). For this experiment, the ions underwent between 385 and 398 ITs in order to most effectively separate the tin ions from isobaric contaminants. After completing their flight, the ions are ejected from the analyzer by opening the mirror closest to the detector. An ETP MagneTOF™ (ETP Electron Multipliers Proprietary Limited, Clyde, New South Wales, Australia) measures the time of flight (TOF) of the ions. The measured TOF is used to deduce the mass via

$$\frac{m}{z} = \frac{c \cdot (t - t_0)^2}{(1 + N_{IT} \cdot b)} \tag{1}$$

with z being the charge state, c, b, and t_0 being calibration parameters, and N_{IT} is the number of isochronous turns. Tune-specific parameters c and t_0 were determined prior to the experiment with well-known, stable ions. For the described experiment, $^{133}Cs^+$ from the MR-TOF MS thermal ion source was utilized and merged with the RIB via the RF switch-yard. For the determination of b, a time-resolved calibration (TRC) [20] is performed using a high-statistics reference peak, which corrects drifts in the Time-of-Flight spectra caused by, for example, diurnal temperature cycles in the experimental hall. TRCs further improve the achievable resolving power and, therefore, the separation of the ion of interest (IOI) from the contamination inherent to RIB production.

To reduce contamination, ions can be mass-selectively retrapped [14]. Once ions are temporally separated in the analyzer, the IOIs are retrapped in the injection trap while the contaminants are deflected. The ions from the injection trap are re-cooled and re-injected into the analyzer, complete another TFS and more ITs, and are ejected for mass measurement. In the tin experiment, the dominant contaminants were atomic In^+, Pd^+, and Ag^+ as well as molecular $Zr^{16}O^+$, $Sr^{19}F^+$, and $Y^{16}O^+$, as seen in Figure 2, where the detected rate was as low as 0.02 particles per second (pps) for $^{104}Sn^+$.

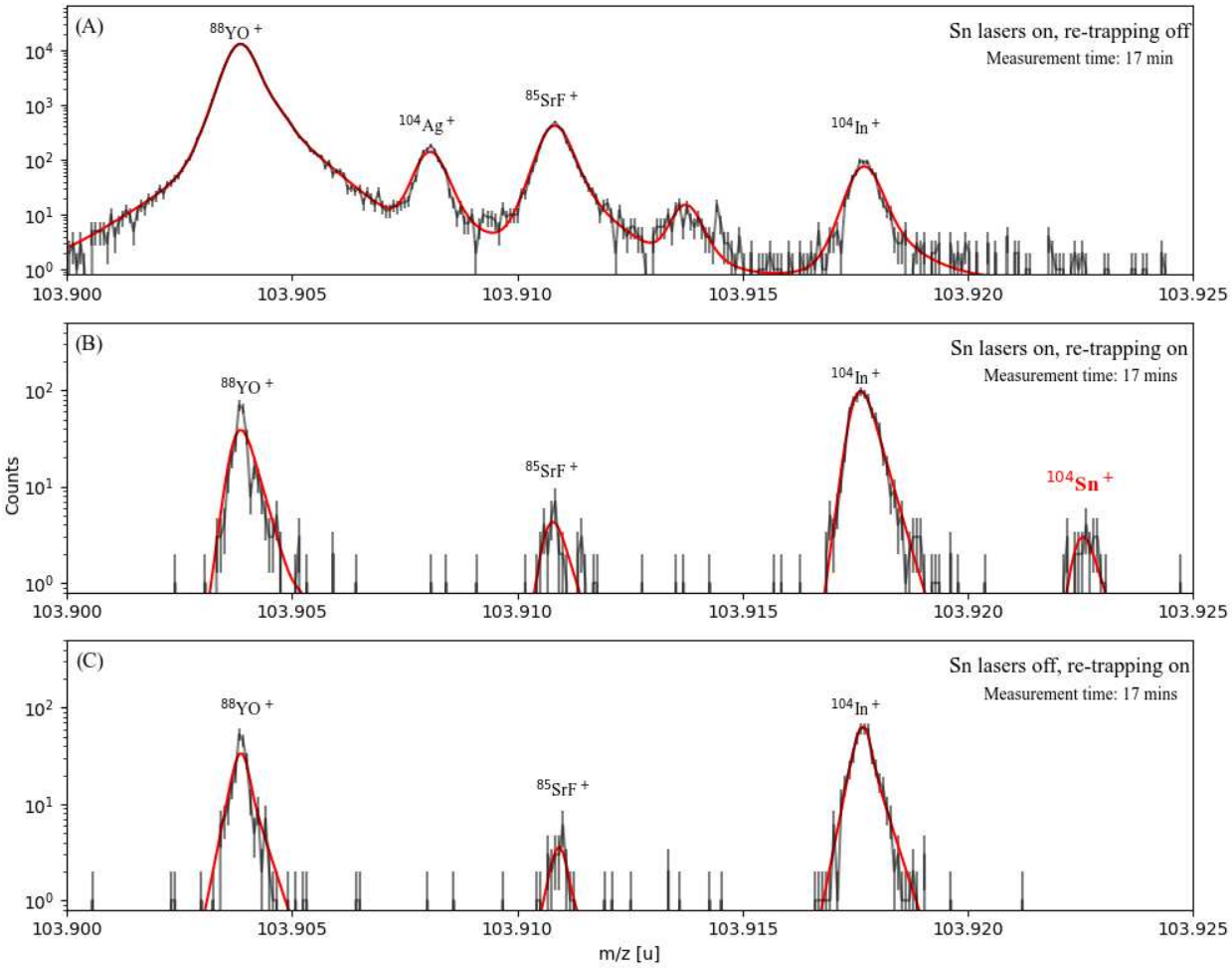

Figure 2. Spectra showing the effects of in situ beam purification by retrapping (off: (**A**); on: (**B**,**C**)) and Sn-ionizing laser beams (blocked: (**C**); unblocked: (**A**,**B**)) at $A = 104$. Without retrapping, the tin isotopes cannot be observed, while the lasers provide an additional elemental confirmation of their identity.

In cases like this tin experiment, the elemental selectivity of TRILIS unambiguously reaffirms the identity of the IOI by comparing spectra with the lasers on and off. In Figure 2

panel C, the peak of ^{104}Sn completely disappears in the absence of its resonant ionization by lasers.

3. Data Analysis

The data analysis follows the procedure described in [20] and is performed in two stages. First, TOF Control software [21] is used to obtain the time-resolved calibration. Spectra are broken down into calibration blocks and the peak of a well-known species in each block is fit with a Gaussian distribution and as a result, the time-dependent constant b is determined for each block.

Second, a fitting package, emgfit [22], employs Exponentially Modified Gaussian (hyper-EMG) distributions [20] for peak fitting. For each mass spectra, a well-resolved, high-statistics peak was selected to be the peak shape calibrant. For this analysis, isobaric $^{g}In^{+}$ was chosen. Since the $^{g}In^{+}$ peaks were broadened due to non-resolved isomers ($^{m}In^{+}$), the spacing between $^{g}In^{+}$ and $^{m}In^{+}$ was a fixed parameter in the fitting procedure [23]. The shape calibrant was individually fit using Pearson's chi-squared statistic, minimizing the χ^2_P cost function. The shape-calibrant peak was fit with hyper-EMG distributions. Then, all of the peaks in the spectra were fit with the Poisson maximum likelihood estimation method (MLE). Here, MLE was preferred over chi-squared due to chi-squared biasing the mean in instances of low counts whereas MLE remained unbiased by implicitly assuming a Poisson distribution.

The ionic mass values, m_{ion}, were determined by

$$m_{\text{ion}} = \frac{(m/z)_{\text{cal,lit}}}{(m/z)_{\text{cal,MLE}}} \cdot (m/z)_{\text{MLE}} \cdot z \tag{2}$$

where $(m/z)_{\text{cal,lit}}$ is the literature mass obtained from AME2020 of the calibrant, $(m/z)_{\text{cal,MLE}}$ is the fitted mass of the calibrant, $(m/z)_{\text{MLE}}$ is the fitted mass of the ion of interest, and z is the charge state of the ion. The mass calibrants for this analysis are specified as "Mass Calibrant" in Table 1. The electron binding energies are negligible (as they are on the order of tens of electron volts) relative to the statistical uncertainty. Lastly, the atomic mass excess ME was determined by

$$ME = m_{\text{ion}} + z \cdot m_e - A \cdot u \tag{3}$$

where m_e is the mass of an electron, A is the mass number (total number of protons and neutrons), and u is the atomic mass unit.

The mass uncertainties were determined by quadratically summing the uncertainty from the fitting procedure to the systematic uncertainty. The systematic error, determined offline to be $\delta m/m = 3 \times 10^{-7}$, was dominated by the (voltage) ringing of the detector-side mirror's electrodes, which could have affected the extraction potential towards the detector. Any effect from ion–ion interactions inside the MR-TOF MS was negligible, as the measurements were performed with one ion per cycle.

Table 1. Summary of the mass excess ME values determined in this work and comparison to literature values obtained from AME2020 [24]. Number of detected events, calibrant species, and ionic mass ratios are presented.

Nuclide	Number of Events	Ionic Mass Ratio *	Mass Calibrant	ME_{TITAN} (keV)	ME_{AME} (keV)	Difference (keV)
^{89}Zr	448	1.00002898 (488)	$^{89}Y^{16}O$	−84,883 (35)	−84,878 (3)	5.2 (35)
^{90g}Y	370	1.000023135 (558)	$^{90}Zr^{16}O$	−86,498 (40)	−86,497 (0.4)	0.6 (40)
^{90m}Y	266	1.000030123 (563)	$^{90}Zr^{16}O$	−85,805 (41)	−85,815 (0.4)	10 (41)

Table 1. *Cont.*

Nuclide	Number of Events	Ionic Mass Ratio *	Mass Calibrant	ME_{TITAN} (keV)	ME_{AME} (keV)	Difference (keV)
^{91g}Y	36,797	1.000015435 (464)	$^{90}Zr^{91}O$	−86,351 (33)	−86,351 (2)	0.7 (33)
^{91m}Y	9328	1.000021048 (476)	$^{90}Zr^{16}O$	−85,797 (35)	−85,796 (2)	1 (35)
^{104}Sn	101	1.00018007 (624)	$^{88}Y^{16}O$	−71,601 (50)	−71,627 (6)	26 (50)
^{105}Sn	626	1.000195519 (483)	$^{89}Y^{16}O$	−73,349 (34)	−73,338 (4)	11 (34)
^{106}Sn	776	1.000164119 (546)	$^{90}Zr^{16}O$	−77,327 (37)	−77,354 (5)	26 (37)
^{107}Sn	350	1.000141815 (476)	$^{91}Zr^{16}O$	−78,511 (34)	−78,512 (5)	1 (34)

* Ionic mass ratios were determined from $m_{IOI}/m_{cal.}$. For ^{A}Y and ^{A}Zr, since they were measured in molecular form, this ratio was determined using the ionic mass of the molecule of interest divided by the ionic mass of the molecular calibrant (e.g., $m_{^{89}Zr^{16}O^{+}}/m_{^{89}Y^{16}O^{+}}$). Errors in ionic mass ratios are given to their decimal place e.g., $1.00002898\ (488) = 1.00002898 \pm 0.00000488$.

4. Results

The mass values for exotic $^{104-107}$Sn are detailed in Table 1 and compared to the AME2020 [24] values. The TITAN and evaluated [24] tin values are found to be in excellent agreement (<1σ), with the latter based on Penning-trap mass determinations [25,26]. A comparison of the two ion-trap methodologies leads to two conclusions. First, the MR-TOF MS achieves a superior speed, sensitivity, and dynamic range, as has been demonstrated at TITAN (e.g., this work) and elsewhere (e.g., [27,28]). Second, while Penning trap mass spectrometry can achieve vastly superior precision, MR-TOF MS achieves sufficient precision for nuclear structure and astrophysics investigations.

To demonstrate the precision required for nuclear structure studies, we calculated the two-neutron separation energy S_{2n} of the relevant tin isotopes:

$$S_{2n} = M(Z, N-2) - M(Z, N) + 2M_n \quad (4)$$

where M_n is the mass of a neutron. In general, S_{2n} ranges from zero (neutron dripline) to tens of MeV (proton dripline), see e.g., Figure 3 of the tin region of interest. The typical behavior of the S_{2n} topology can be most easily understood through the nuclear shell model [29], wherein dramatically more stability is found at certain occupation (or "magic") numbers like neutron numbers N = 2, 8, 20, 28, 50, 82, and 126. Partially filled shells manifest as a near-linear trend in S_{2n}, a sharp discontinuity at closed shells, and more complicated behavior for highly deformed nuclei. The uncertainties achieved in this TITAN MR-TOF MS experiment (and all others) are adequate to probe nuclear shells and the evolution of the nuclear structure towards the driplines.

Success in measuring highly exotic species towards or at the driplines depends on the sensitivity of the MR-TOF MS. The lowest rate of detected ions in the tin experiment is 0.02 pps and in other TITAN experiments, down to 0.0007 pps [5]. This sensitivity is, in large part, due to the in situ beam purification or retrapping method (described above), which can, in milliseconds, remove decades of contamination. While TITAN practice is to aim for at least 10 ions per IOI peak, as little as one ion suffices [27] and underscores the importance single-ion sensitivity and methodologies in addition to beam purification. As such, the MR-TOF MS can capture high RIB rates, purify the IOI (Figure 2), and then perform the mass measurement without ion–ion interactions.

Contamination poses two obstacles: obscuring the IOI and introducing a systematic shift in the measured mass due to ion–ion interactions. In the tin experiment, retrapping reduced the maximum ratio of IOI to contamination from about 1:10^2 to, at most, 1:30 (e.g., see Figure 2A,B). For more typical retrapping scenarios, the dynamic range exceeds the

space-charge limit of any precision Penning trap mass spectrometer [30] and can only be matched by TOF spectrometers [31,32]. The former often relies on identifying contaminants on-line and then cleaning them individually (see [30] and references therein). As such, substantial time is lost to preparing (rather than measuring) the IOI. The latter can sustain a high space charge, is broadband, and can be divided into so-called Bρ-TOF and storage-ring-based measurements. Bρ-TOF can reach a single-ion sensitivity and precision similar to those of MR-TOF; however, the complexity of the calibration, oftentimes requiring many well-known masses, can pose a significant challenge. For TOF experiments in a storage ring to achieve single-ion sensitivity and a precision comparable to that of MR-TOF, the required beam cooling raises the lower limit of the half-life to the order of one second, about 200 times higher than that demonstrated in the TITAN MR-TOF MS, of 6 ms [4].

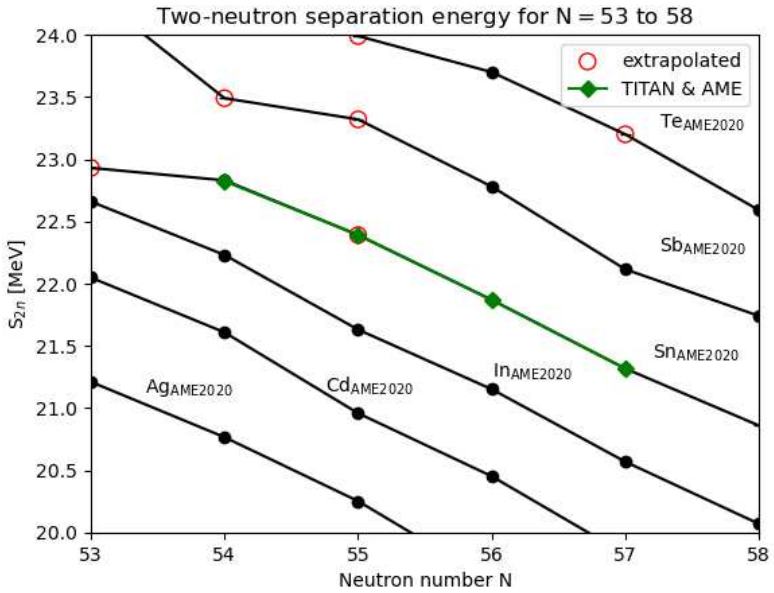

Figure 3. Surveys of the two-neutron separation energy S_{2n} are a common method to examine the evolution of nuclear structure; as the vertical axis scale indicates, the desired precision is less than about 100 keV, well within reach of the MR-TOF MS. The TITAN values have been combined with AME values in this plot, seen in green, with a variance weighted mean. Red circles indicate values extrapolated from the mass surface by the authors of AME2020.

Capable of measuring species with half-lives of a few ms, the MR-TOF MS is well suited to measurements approaching the driplines, although, in the neutron-deficient Sn isotopes, the half-lives range from a few to tens of seconds due to their "magic" nature (of the closed proton shell). The half-life (here, at least 21 s for ^{104}Sn [23]) along with the expected yield and contamination rate determine the MR-TOF MS duty cycle prepared for each experiment. The short duty cycles and the sensitivity allow for fast measurements; the duration of this experiment was about 10 h, with the complete data being collected in a mere four hours.

5. Discussion on Direct and Indirect Mass Measurements

In the tin isotopes, the neutron-deficient isotope of ^{103}Sn had only been measured indirectly through its β-endpoint energy [33,34]. Both measurements have been discarded by the AME2020 authors (see pp. 21–22 of [35] for the full discussion) because the trends in the mass surface indicate ^{103}Sn should be 120 keV more bound. In β-endpoint energy measurements, systematic errors like the pandemonium effect [36] can be significant. This example underscores the need for accuracy, typically best achieved by direct techniques.

For this reason, we present herein the first direct mass measurements of ^{89}Zr and ^{90,91}Y, with an example spectra seen in Figure 4.

In comparing the neighborhood of ^{89}Zr and ^{90,91}Y with that of $^{104–107}$Sn in Figure 5, their simultaneous measurement may appear unlikely. However, the Zr and Y formed oxide molecules and were delivered to TITAN as molecular ions; consequently, they were isobars of the tin IOI. Their simultaneous measurement was enabled by the broadband or non-resonant nature of MR-TOF MS. (The molecular bond is negligible relative to the statistical uncertainty.) In all three cases, good agreement was found between the TITAN and AME2020 values, and the TITAN ^{91}Y value shows a modest improvement on future mass evaluations. This experiment demonstrates how the contamination inherent to RIB production may allow for additional measurements of nuclides, which were formerly known only by indirect measurements (this work) or can anchor a chain of indirect measurements [15]. Surprisingly, many nuclides near stability have been measured only indirectly (see Figure 5) despite their value in verifying trends in the mass surface and therefore our understanding in nuclear structure.

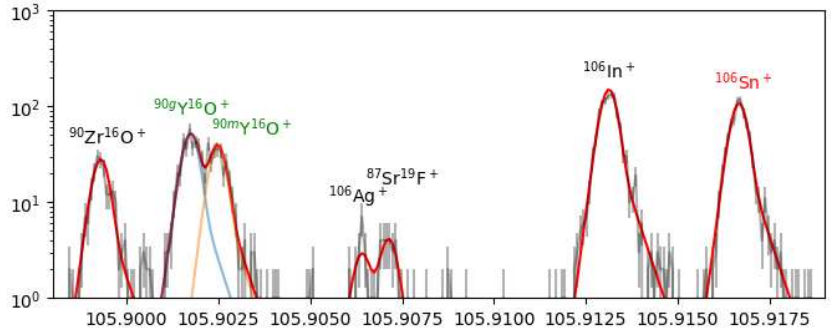

Figure 4. Spectra at mass number $A = 106$ showing the first direct mass measurement of $^{90}Y^+$, along with the isotope of interest, $^{106}Sn^+$. Orange and blue line shapes indicate the individual fits of the ground and excited states of $^{90}Y^+$ that were observed, with the summed line shape indicated in red. This simultaneous measurement was achievable due to the broadband capabilities of the MR-TOF technique.

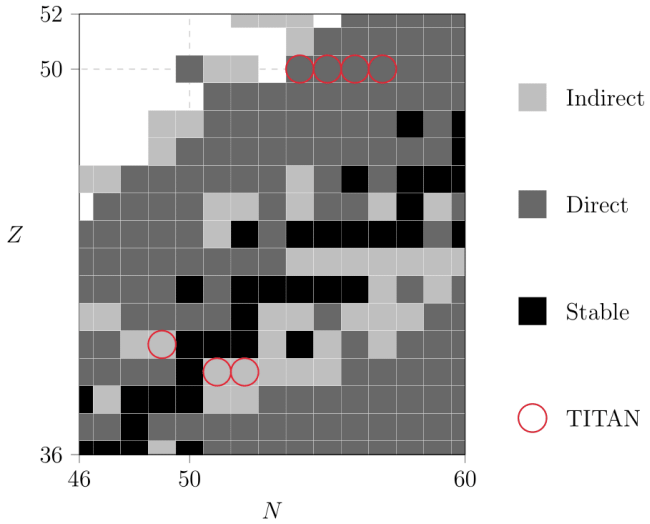

Figure 5. The section of the chart of nuclides relevant to this article displayed by measurement type listed in the AME2020 [24]; see text for more information. Tens of nuclides have had their masses measured only indirectly (light gray) despite being adjacent to the so-called "valley of stability". Three of these—^{89}Zr and ^{90,91}Y—have been measured in this work (red circles), despite the focus on the neutron-deficient tin isotopes. These measurements were possible due to the broadband nature of the MR-TOF MS.

6. Summary and Outlook

High-precision mass measurements of neutron-deficient tin isotopes as well as first-time direct measurements of ^{89}Zr and ^{90,91}Y were performed at TITAN-TRIUMF using the MR-TOF MS technique. All results confirmed the AME2020 values within 1σ in only four hours of measurement time, a fraction of the time required for Penning trap mass spectrometry, which was previously used to explore this region.

The experiment showcases the capabilities of the MR-TOF MS to meet the challenges of surveying towards and along the nuclear driplines: duty cycles compatible with half-lives of only a couple milliseconds; at TITAN, half-lives as low as 6 ms have been measured. High resolving powers separate the species of interest from contaminants; at TITAN, resolving powers up to 600,000 have been demonstrated [37] with ongoing efforts for higher values. Finally, retrapping permits a dynamic range as large as $1{:}10^8$ to measure species with detected rates as low as 0.0007 pps. Finally, MR-TOF MS is a broadband, non-resonant technique that can allow for the simultaneous mass cartography of nearby regions of interest. These factors and a typical precision of $\sim 10^{-7}$ make the MR-TOF MS an ideal instrument to survey the driplines. Such measurements are of the highest priority to understand the evolution of nuclear structure and explosive nucleosynthesis, where sensitivity, precision, and accuracy are critical.

Author Contributions: Data curation, J.B. and S.F.P.; formal analysis, A.C.; funding acquisition, T.B., J.D., M.P.R. and A.A.K.; investigation, S.B., E.D., J.F., D.F., L.G., Z.H., C.I., A.J., B.K., Y.L., E.L., E.M.L., I.M., S.F.P., M.P.R., J.L.T.J. and A.A.K.; software, J.B., S.F.P., W.R.P. and C.S.; supervision, T.B. and A.A.K.; validation, F.M.M., A.M. and M.P.R.; visualization, C.L.B. and A.C.; writing—original draft, A.C.; writing—review and editing, C.L.B., A.C., T.D., E.D., J.F., B.K., S.M.-E., F.M.M., A.M., E.L., E.M.L., W.R.P., M.P.R., C.S. and A.A.K. All authors with current contact information have read and agreed to the published version of the manuscript.

Funding: This work was funded by the Natural Sciences and Engineering Research Council (NSERC) of Canada and the National Research Council (NRC) of Canada through TRIUMF as well as from the German Federal Ministry for Education and Research (BMBF) under contracts no. 05P19RGFN1 and 05P21RGFN1, the German Research Foundation (DFG) under contract no. 422761894, by HGS-HIRe, by Justus-Liebig-Universität Gießen and GSI under the JLU-GSI strategic Helmholtz partnership agreement.

Data Availability Statement: The data supporting the conclusions of this article can be made available by the authors on request.

Acknowledgments: The author wishes to acknowledge and thank Mel Good for his expertise in maintaining the TITAN facility and Jens Lassen and the TRIUMF laser group for their outstanding work in creating laser schemes and for their tireless hard work.

Conflicts of Interest: The funders had no role in the design of the study; in the collection, analyses, or interpretation of the data; in the writing of the manuscript; or in the decision to publish the results.

Abbreviations

The following abbreviations are used in this manuscript:

AME	Atomic Mass Evaluation
EMG	Exponentially Modified Gaussian
IOI	Ion(s) of interest
ISOL	Isotope Separation On-Line
IT	Isochronous turn(s)
MLE	Maximum Likelihood Estimator
MR-TOF MS	Multiple-Reflection Time-of-Flight Mass Spectrometer
PPS	Particles per second

RFQ	Radio Frequency Quadrupole
RIB	Radioactive ion beam
TFS	Time Focus Shift
TITAN	TRIUMF's Ion Trap for Atomic and Nuclear science
TOF	Time-of-Flight
TRC	Time-resolved calibration
TRILIS	TRIUMF's Resonant Ionization Laser Ion Source

References

1. Reiter, M.; Andrés, S.; Bergmann, J.; Dickel, T.; Dilling, J.; Jacobs, A.; Kwiatkowski, A.; Plaß, W.; Scheidenberger, C.; Short, D.; et al. Commissioning and performance of TITAN's Multiple-Reflection Time-of-Flight Mass-Spectrometer and isobar separator. *Nucl. Instrum. Methods Phys. Res. Sect. A Accel. Spectrometers Detect. Assoc. Equip.* **2021**, *1018*, 165823. Available online: http://www.sciencedirect.com/science/article/pii/S0168900221008081 (accessed on 14 July 2023). [CrossRef]
2. Jesch, C.; Dickel, T.; Plaß, W.R.; Short, D.; Ayet San Andres, S.; Dilling, J.; Geissel, H.; Greiner, F.; Lang, J.; Leach, K.; et al. The MR-TOF-MS isobar separator for the TITAN facility at TRIUMF. *Hyperfine Interact.* **2015**, *235*, 97–106. [CrossRef]
3. Kwiatkowski, A.A.; Dilling, J.; Malbrunot-Ettenauer, S.; Reiter, M. 15 years of precision mass measurements at TITAN. *Eur. Phys. J.* **2024**, *60*, 87. [CrossRef]
4. Lykiardopoulou, E.; Walls, C.; Bergmann, J.; Brodeur, M.; Brown, C.; Cardona, J.; Czihaly, A.; Dickel, T.; Duguet, T.; Ebran, J.; et al. Refined topology of the N = 20 island of inversion with high precision mass measurements of Na and Mg. *Phys. Rev. Lett.* **2025**. Available online: https://journals.aps.org/prl/accepted/9f07aY98Gc61f69ec067770872dfd0a083489ceff (accessed on 27 July 2024).
5. Paul, S.; Bergmann, J.; Cardona, J.; Dietrich, K.; Dunling, E.; Hockenbery, Z.; Hornung, C.; Izzo, C.; Jacobs, A.; Javaji, A.; et al. Mass measurements of $^{60-63}$Ga reduce x-ray burst model uncertainties and extend the evaluated T = 1 isobaric multiplet mass equation. *Phys. Rev. C* **2021**, *104*, 065803. [CrossRef]
6. Dickel, T.; Plaß, W.; Becker, A.; Czok, U.; Geissel, H.; Haettner, E.; Jesch, C.; Kinsel, W.; Petrick, M.; Scheidenberger, C.; et al. A high-performance multiple-reflection time-of-flight mass spectrometer and isobar separator for the research with exotic nuclei. *Nucl. Instrum. Methods Phys. Res. Sect. A Accel. Spectrometers Detect. Assoc. Equip.* **2015**, *777*, 172–188. Available online: https://www.sciencedirect.com/science/article/pii/S0168900214015629 (accessed on 12 August 2024). [CrossRef]
7. Yavor, M.; Plaß, W.; Dickel, T.; Geissel, H.; Scheidenberger, C. Ion-optical design of a high-performance multiple-reflection time-of-flight mass spectrometer and isobar separator. *Int. J. Mass Spectrom.* **2015**, *381–382*, 1–9. Available online: https://www.sciencedirect.com/science/article/pii/S1387380615000202 (accessed on 12 August 2024). [CrossRef]
8. Plaß, W.; Dickel, T.; Czok, U.; Geissel, H.; Petrick, M.; Reinheimer, K.; Scheidenberger, C.; Yavor, M.I. Isobar separation by time-of-flight mass spectrometry for low-energy radioactive ion beam facilities. *Nucl. Instrum. Methods Phys. Res. Sect. B Beam Interact. Mater. Atoms* **2008**, *266*, 4560–4564. Available online: https://www.sciencedirect.com/science/article/pii/S0168583X08007763 (accessed on 12 August 2024). [CrossRef]
9. Schury, P.; Okada, K.; Shchepunov, S.; Sonoda, T.; Takamine, A.; Wada, M.; Wollnik, H.; Yamazaki, Y. Multi-reflection time-of-flight mass spectrograph for short-lived radioactive ions. *Eur. Phys. J. A* **2009**, *42*, 343–349. [CrossRef]
10. Wolf, R.; Eritt, M.; Marx, G.; Schweikhard, L. A multi-reflection time-of-flight mass separator for isobaric purification of radioactive ion beams. *Hyperfine Interact.* **2011**, *199*, 115–122. [CrossRef]
11. Mardor, I.; Andrés, S.; Dickel, T.; Amanbayev, D.; Beck, S.; Bergmann, J.; Geissel, H.; Gröf, L.; Haettner, E.; Hornung, C.; et al. Mass measurements of As, Se, and Br nuclei, and their implication on the proton-neutron interaction strength toward the N = Z line. *Phys. Rev. C* **2021**, *103*, 034319. [CrossRef]
12. Jacobs, A.; Andreoiu, C.; Bergmann, J.; Brunner, T.; Dickel, T.; Dillmann, I.; Dunling, E.; Flowerdew, J.; Graham, L.; Gwinner, G.; et al. Improved high-precision mass measurements of mid-shell neon isotopes. *Nucl. Phys. A* **2023**, *1033*, 122636. Available online: https://www.sciencedirect.com/science/article/pii/S0375947423000398 (accessed on 5 July 2024). [CrossRef]
13. Leistenschneider, E.; Dunling, E.; Bollen, G.; Brown, B.; Dilling, J.; Hamaker, A.; Holt, J.; Jacobs, A.; Kwiatkowski, A.; Miyagi, T.; et al. Precision Mass Measurements of Neutron-Rich Scandium Isotopes Refine the Evolution of N = 32 and N = 34 Shell Closures. *Phys. Rev. Lett.* **2021**, *126*, 042501. [CrossRef] [PubMed]
14. Beck, S.; Kootte, B.; Dedes, I.; Dickel, T.; Kwiatkowski, A.; Lykiardopoulou, E.; Plaß, W.; Reiter, M.; Andreoiu, C.; Bergmann, J.; et al. Mass Measurements of Neutron-Deficient Yb Isotopes and Nuclear Structure at the Extreme Proton-Rich Side of the N = 82 Shell. *Phys. Rev. Lett.* **2021**, *127*, 112501. [CrossRef] [PubMed]
15. Lykiardopoulou, E.; Audi, G.; Dickel, T.; Huang, W.; Lunney, D.; Plaß, W.; Reiter, M.; Dilling, J.; Kwiatkowski, A. Exploring the limits of existence of proton-rich nuclei in the Z = 70–82 region. *Phys. Rev. C* **2023**, *107*, 024311. [CrossRef]

16. Bricault, P.; Baartman, R.; Dombsky, M.; Hurst, A.; Mark, C.; Stanford, G.; Schmor, P. TRIUMF-ISAC target station and mass separator commissioning. *Nucl. Phys. A* **2002**, *701*, 49–53. Available online: https://www.sciencedirect.com/science/article/pii/S0375947401015469 (accessed on 12 July 2024). [CrossRef]
17. Lassen, J.; Bricault, P.; Dombsky, M.; Lavoie, J.; Gillner, M.; Gottwald, T.; Hellbusch, F.; Teigelhöfer, A.; Voss, A.; Wendt, K. Laser Ion Source Operation at the TRIUMF Radioactive Ion Beam Facility. *AIP Conf. Proc.* **2009**, *1104*, 9–15. [CrossRef]
18. Brunner, T.; Smith, M.; Brodeur, M.; Ettenauer, S.; Gallant, A.; Simon, V.; Chaudhuri, A.; Lapierre, A.; Mané, E.; Ringle, R.; et al. TITAN's digital RFQ ion beam cooler and buncher, operation and performance. *Nucl. Instrum. Methods Phys. Res. Sect. A Accel. Spectrometers Detect. Assoc. Equip.* **2012**, *676*, 32–43. Available online: https://www.sciencedirect.com/science/article/pii/S0168900212001398 (accessed on 18 July 2023). [CrossRef]
19. Plaß, W.; Dickel, T.; Andres, S.; Ebert, J.; Greiner, F.; Hornung, C.; Jesch, C.; Lang, J.; Lippert, W.; Majoros, T.; et al. High-performance multiple-reflection time-of-flight mass spectrometers for research with exotic nuclei and for analytical mass spectrometry. *Phys. Scr.* **2015**, *T166*, 014069. [CrossRef]
20. Ayet San Andrés, S.; Hornung, C.; Ebert, J.; Plaß, W.; Dickel, T.; Geissel, H.; Scheidenberger, C.; Bergmann, J.; Greiner, F.; Haettner, E.; et al. High-resolution, accurate multiple-reflection time-of-flight mass spectrometry for short-lived, exotic nuclei of a few events in their ground and low-lying isomeric states. *Phys. Rev. C* **2019**, *99*, 064313. [CrossRef]
21. Dickel, T.; San Andres, S.; Beck, S.; Bergmann, J.; Dilling, J.; Greiner, F.; Hornung, C.; Jacobs, A.; Kripko-Koncz, G.; Kwiatkowski, A.; et al. Recent upgrades of the multiple-reflection time-of-flight mass spectrometer at TITAN, TRIUMF. *Hyperfine Interact.* **2019**, *240*, 62. [CrossRef]
22. Paul, S. *emgfit-Fitting of Time-of-Flight Mass Spectra with Hyper-EMG Models*; Zenodo: Geneva, Switzerland, 2024; Volume 1. [CrossRef]
23. Kondev, F.; Wang, M.; Huang, W.; Naimi, S.; Audi, G. The NUBASE2020 evaluation of nuclear physics properties. *Chin. Phys. C* **2021**, *45*, 030001. [CrossRef]
24. Wang, M.; Huang, W.; Kondev, F.; Audi, G.; Naimi, S. The AME 2020 atomic mass evaluation (II). Tables, graphs and references *. *Chin. Phys. C* **2021**, *45*, 030003. [CrossRef]
25. Martin, A.; Ackermann, D.; Audi, G.; Blaum, K.; Block, M.; Chaudhuri, A.; Di, Z.; Eliseev, S.; Ferrer, R.; Habs, D.; et al. Mass measurements of neutron-deficient radionuclides near the end-point of the rp-process with SHIPTRAP. *Eur. Phys. J. A* **2007**, *34*, 341–348. [CrossRef]
26. Elomaa, V.; Vorobjev, G.; Kankainen, A.; Batist, L.; Eliseev, S.; Eronen, T.; Hakala, J.; Jokinen, A.; Moore, I.; Novikov, Y.; et al. Quenching of the SnSbTe Cycle in the rp Process. *Phys. Rev. Lett.* **2009**,*102*, 252501. [CrossRef] [PubMed]
27. Schury, P.; Wada, M.; Ito, Y.; Kaji, D.; Arai, F.; MacCormick, M.; Murray, I.; Haba, H.; Jeong, S.; Kimura, S.; et al. First online multireflection time-of-flight mass measurements of isobar chains produced by fusion-evaporation reactions: Toward identification of superheavy elements via mass spectroscopy. *Phys. Rev. C* **2017**, *95*, 011305. [CrossRef]
28. Wienholtz, F.; Beck, D.; Blaum, K.; Borgmann, C.; Breitenfeldt, M.; Cakirli, R.; George, S.; Herfurth, F.; Holt, J.; Kowalska, M.; et al. Masses of exotic calcium isotopes pin down nuclear forces. *Nature* **2013**, *498*, 346–349. Available online: http://EconPapers.repec.org/RePEc:nat:nature:v:498:y:2013:i:7454:d:10.1038_nature12226 (accessed on 9 May 2024). [CrossRef] [PubMed]
29. Mayer, M. On Closed Shells in Nuclei. II. *Phys. Rev.* **1949**, *75*, 1969–1970. [CrossRef]
30. Ascher, P.; Daudin, L.; Flayol, M.; Gerbaux, M.; Grévy, S.; Hukkanen, M.; Husson, A.; Roubin, A.; Alfaurt, P.; Blank, B.; et al. PIPERADE: A double Penning trap for mass separation and mass spectrometry at DESIR/SPIRAL2. *Nucl. Instrum. Methods Phys. Res. Sect. A Accel. Spectrometers Detect Assoc. Equip.* **2021**, *1019*, 165857. Available online: https://www.sciencedirect.com/science/article/pii/S0168900221008421 (accessed on 14 April 2024). [CrossRef]
31. Blaum, K. High-accuracy mass spectrometry with stored ions. *Phys. Rep.* **2006**, *425*, 1–78. Available online: https://www.sciencedirect.com/science/article/pii/S0370157305004643 (accessed on 6 June 2024). [CrossRef]
32. Meisel, Z.; George, S. Time-of-flight mass spectrometry of very exotic systems. *Int. J. Mass Spectrom.* **2013**, *349–350*, 145–150. Available online: https://www.sciencedirect.com/science/article/pii/S1387380613001139 (accessed on 10 March 2024). [CrossRef]
33. Mukha, I.; Batist, L.; Becker, F.; Blazhev, A.; Brüchle, A.; Döring, J.; Górska, M.; Grawe, H.; Faestermann, T.; Hoffman, C.; et al. Studies of β-delayed proton decays of N ≃ Z nuclei around ^{100}Sn at the GSI-ISOL facility. *Nucl. Phys. A* **2004**, *746*, 66–70. Available online: https://www.sciencedirect.com/science/article/pii/S0375947404009674 (accessed on 21 June 2024). [CrossRef]
34. Kavatsyuk, O.; Kavatsyuk, M.; Batist, L.; Banu, A.; Becker, F.; Blazhev, A.; Brüchle, W.; Döring, J.; Faestermann, T.; Górska, M.; et al. Beta decay of 103Sn. *Eur. Phys. J. A Hadron. Nucl.* **2005**, *25*, 211–222 (accessed on 21 June 2024). [CrossRef]
35. Huang, W.; Wang, M.; Kondev, F.; Audi, G.; Naimi, S. The AME 2020 atomic mass evaluation (I). Evaluation of input data, and adjustment procedures. *Chin. Phys. C* **2021**, *45*, 030002. [CrossRef]

36. Hardy, J.; Carraz, L.; Jonson, B.; Hansen, P. The essential decay of pandemonium: A demonstration of errors in complex beta-decay schemes. *Phys. Lett. B*. **1977**, *71*, 307–310. Available online: https://www.sciencedirect.com/science/article/pii/0370269377902234 (accessed on 21 June 2024). [CrossRef]
37. Porter, W.; Ashrafkhani, B.; Bergmann, J.; Brown, C.; Brunner, T.; Cardona, J.; Curien, D.; Dedes, I.; Dickel, T.; Dudek, J.; et al. Mapping the N = 40 island of inversion: Precision mass measurements of neutron-rich Fe isotopes. *Phys. Rev. C* **2022**, *105*, L041301. (accessed on 12 July 2023). [CrossRef]